Computational Modeling of Flowin Annular Non-Rotating Pipe

*Mohamed Milad Ahmed**

Department of Petroleum, Faculty of Engineering, Sirte University, Sirte, Libya
E-mail: massiwi@su.edu.ly

Abstract

The flow through annulus with rotation of the inner cylinder is important, and one of its applications is with drilling of oil wells where drilling fluid flows between the drillstring and the well casing or the open hole to transport cuttings to the surface. The drilling fluids usually have non-Newtonian properties and the rheological requirements are that they should have low effective viscosity, consistent with transporting drilled cuttings back to surface, and high effective yield stress to keep solids in suspension during stationary periods]1].

As a first step towards good understanding of flow through annulus with rotation of the inner pipe, a study of flow through the annulus of stationary pipes may became necessary, This paper amid at presenting results of a computational study of steady, compressible flow with different Reynolds numbers through a Axisymmetric geometry, then the computational results was compared with previously experimental work performed by Quarm by 1967]2] for the same geometry and same fluid type and parameters. In the present work the commercial CFD code Fluent v6.0.20]3] is used to compute the results of computational study. Computational results shows that modifying the wall function constants considering experimental values has no great effect on solution accuracy (Fig 5 and 8). Good agreement between computational and experimental results was obtained once the specified flow rates had been corrected, as shown in (Fig 11).

Keywords: Induction machine, diagnostics, current spectrum, harmonics.

Abbreviations and Acronyms

A	Cross-sectional-Area
B	Empirical constant (Law of the Wall)
D	Diameter (mm)
d_e	External diameter of the drill pipe (mm)
E	Empirical constant (Law of the Wall)
k-ε	Turbulence model
k-ω	Turbulence model
Re	Reynolds number
Re_Q	Axial Reynolds Number
r_i	Inner radius (mm)
r_o	Outer radius (mm)
U	x Component of mean flow velocity (m/s)

*Author for correspondence

$\overline{U}$	Average velocity (m/s)
u^+	Dimensionless velocity
u_i^+	Inner wall dimensionless velocity
u_o^+	Outer wall dimensionless velocity
V	y Component of mean flow velocity (m/s)
y^+	Dimensionless distance from wall
y_i^+	Dimensionless distance from the inner wall
y_o^+	Dimensionless distance from the outer wall
CFD	Computational Fluid Dynamics
UDF	User defined functions
Greek	
ν	Kinematic viscosity (m^2/s)
κ	Von Karman's constant (law of the wall)

1. Introduction

Fluid flowing through different geometries of annuli has been experimentally, analytically and computationally studied by many authors, examples of studies of nonrotating Newtonian flows in concentric and eccentric annuli are]2, 4,5,6,7,8, 9 and 10[.

As a preliminary study, a comparison of CFD modeling with a previous experimental investigation by Quarmby [2] for non-swirling developed flow in a concentric annular pipe with Reynolds numbers ranging from 6000 to 90000 and diameter ratio D/de = 5.62 was carried out. Table 1 shows Quarmby cases and the flows parameters being computationally investigated in this work and confirms that these are similar to the flows be studied.

Table 1. Quarmby's experimentally investigated case.

	Quarmby (1967)
D/de	Overall range (2.88 – 9.37)
	D/de Compared = 5.62
$Re = \dfrac{D\overline{U}}{\nu}$	Overall range 14.2×10^3 - 88.6×10^3
	Re Compared 14.2×10^3
$Re_Q = \dfrac{Q}{\upsilon . D\left(1+\frac{d_e}{D}\right)}$	Overall range 14.8×10^3 - 92.2×10^3
	Re Compared 14.8×10^3

Quarmby (1967) experimentally studied a fully developed unidirectional turbulent flow in three vertical and horizontal concentric annuli. The radius ratios were 2.88, 5.62 and 9.37, with air as working fluid and for Reynolds numbers ranging from 6000 to 90,000. Reynolds number:

$$Re = \frac{D\bar{U}}{\nu} \qquad (1)$$

was based on annulus diameter difference:

$$D = 2\,(r_o - r_i) \qquad (2)$$

mean flow velocity:

$$\bar{U} = \int_A U\, dA / A \qquad (3)$$

and kinematic viscosity (ν) of the working fluid. The results presented were examined in terms of development length, friction factor, radius of maximum velocity and velocity profiles. The results show that the hydrodynamic entrance length was found to be much the same as for round tubes. The friction factor was found to be independent of radius ratio within the limits of experimental accuracy. In particular, it was found that the radius of maximum velocity for highly turbulent flow is different from its value for low turbulence flow. The difference was found to be a function of both Reynolds number and radius ratio.

The dimensionless velocity u^+ against dimensionless distance y^+ (Equation 4) from the outer and inner walls is influenced by the Reynolds number. For a given radius ratio, low *Re* has an effect on the inner profile opposite to its effect on the outer profile. In the inner profile the average gradient in u^+_i / y^+_i co-ordinates increases as *Re* increases, but in the outer profile the average gradient in u^+_o / y^+_o co-ordinates decreases as *Re* increases.

$$u^+ = \frac{1}{\kappa} \ln(y^+) + B = \frac{1}{\kappa} \ln(E\, y^+) \qquad (4)$$

2. Computational Modeling

A fully developed flow of a typical vertical annulus of radius ratio of 5.62 was examined by the author employing Fluent code]3]. The velocity profiles were examined in terms of velocity profile shape and position of maximum velocity. Three different models were employed:

A full length solution domain allowing the velocity profile to develop into a fully-developed flow. A short length solution domain using periodic boundary conditions to create a fully developed flow, using both

k-ε turbulence closure and,

k-ω turbulence closure.

3. Full Length Developing Solution Domain

The solution domain is shown in Fig 1. Grid independence for the solution was examined. The meshes examined for the model geometry, of length 6*m* (327 *D*) to ensure fully developed flow, ranged from a relatively coarse mesh of 600 × 5 to a point beyond which the solution was found to be grid independent of 1200 × 14 which was adopted for this computational work.

To ensure fully developed flow, axial velocity profiles for a typical *Re* of 62986 at different positions prior to outlet were plotted. Fig 2 shows that the axial velocities at different locations prior to exit are superimposed over each other indicating fully developed flow. As well, wall shear stresses along the inner and outer walls were constant as shown in Fig 3.

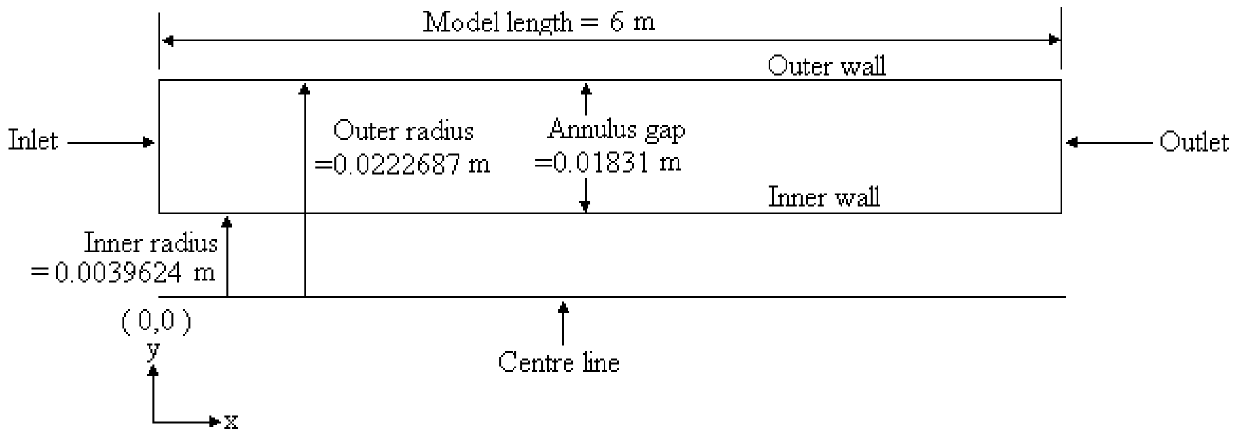

Figure 1. Axisymmetric annular flow solution domain

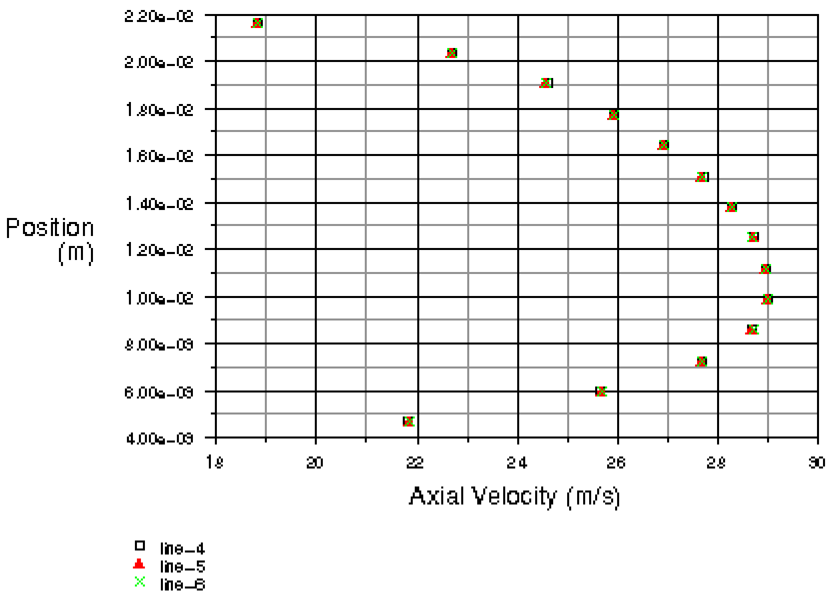

Figure 2. Axial velocity development for a typical *Re* = 62986 shows that the velocity is fully developed at different positions prior to outlet (model full dimensions with standard k-ε).

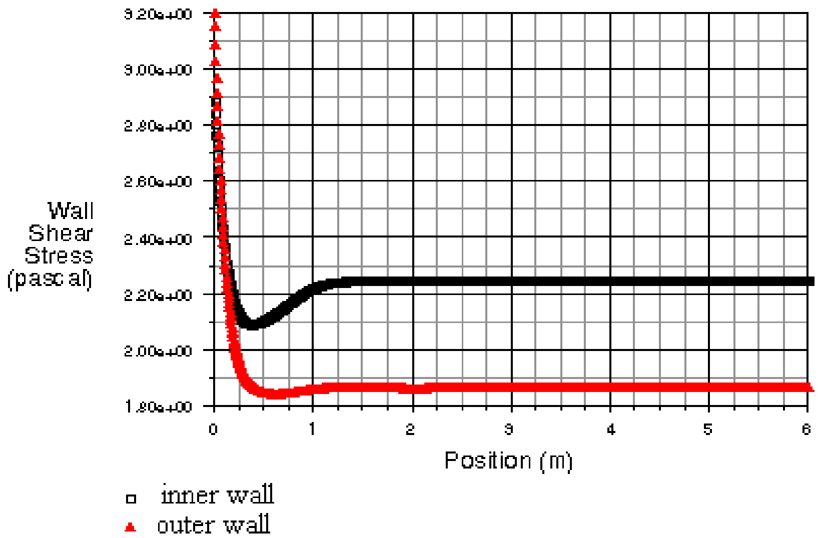

Figure 3. Constant shear stress plot as indication to fully developed flow *Re* = 62986.

Comparison between CFD and Quarmby's results is shown in Fig 4. This shows a disagreement between the two results in terms of the value of maximum velocities and velocity profiles near the inner walls which were pronounced at high Reynolds numbers.

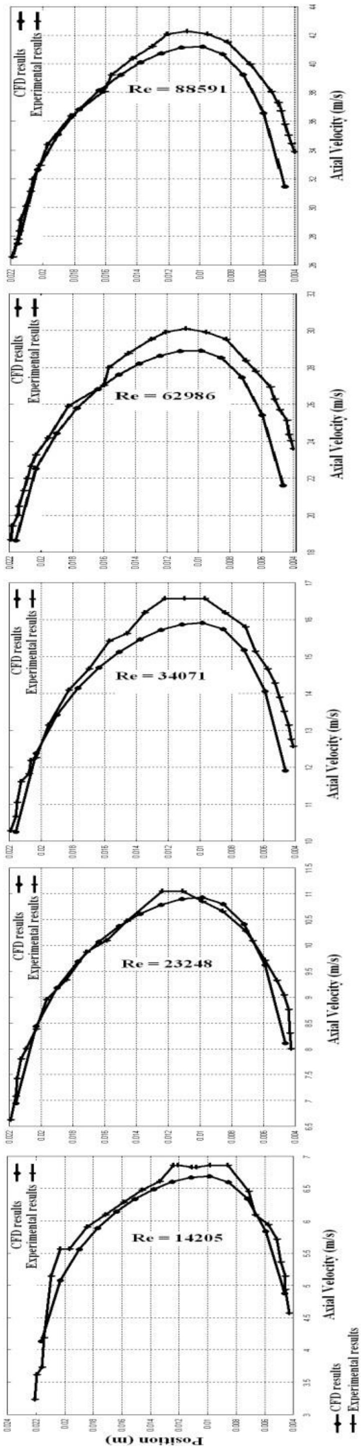

Figure 4. Comparison of experimental defaults and computational results (standard *k*-*ε* results with fluent defaults)

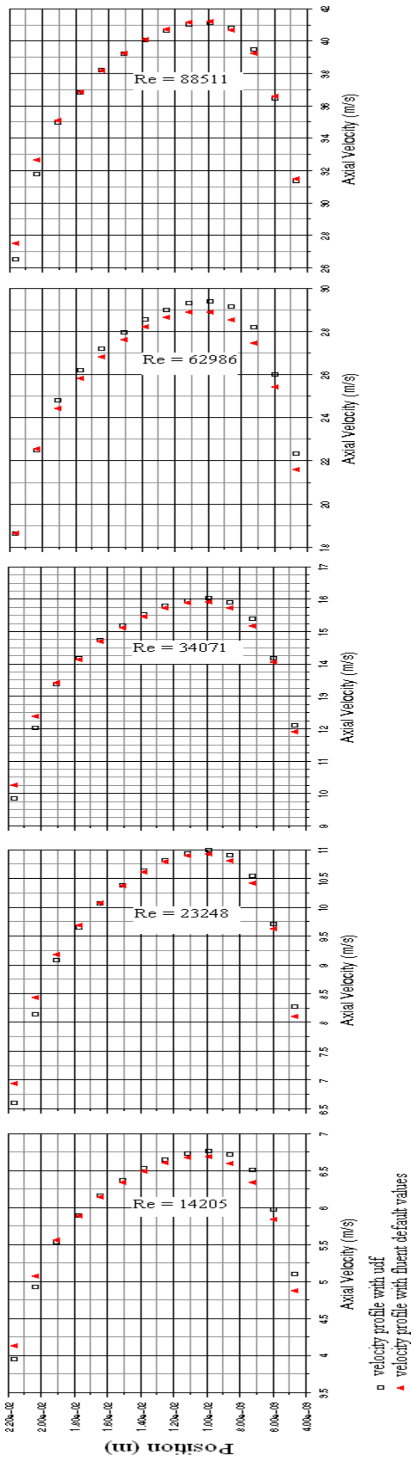

Figure 5. Standard *k*-*ε* with fluent and user defined functions

Inasmuch as mesh independence was examined carefully and the model length was sufficient to ensure fully developed flow, so the inconsistency of results was most likely attributed to either wall functions or volumetric flow error.

As Fluent uses default values for law of the wall [11], so in order to consider changes to the experimental constants for the law of the wall, it is necessary to define these functions into Fluent. Details of creating a UDF file through C programs modeling the experimental values [12], compilation and steps of linkage and running Fluent with UDF are given in [13]. The same Fluent case files used above were run again but this time with Quarmby's suggested experimental constants of law of the wall for inner and outer walls as:

$$u_i^+ = 1.73 \log y_i^+ + 9.4 \qquad (5)$$

and

$$u_o^+ = 2.62 \log y_o^+ + 4.6 \qquad (6)$$

respectively. Regarding these two equations of the law of the wall, the experimental constants entered into Fluent would be E (inner) = 228.8, E (outer) = 5.788 and kappa (inner) = 0.5780 and kappa (outer) = 0.3817.

A comparison between standard k-ε with Fluent default law of the wall and standard k-ε with experimental constants for law of the wall (UDF) results is shown in Fig 5. This shows only a marginal increment of the value of maximum axial velocity. This tells us that the wall functions were not the main cause of the disagreements.

4. Streamwise Periodic (Cyclic) Technique

Fluent provides the ability to calculate either streamwise periodic or developing fluid flow. Examples of streamwise periodic flows include fully developed flow in pipes and ducts. With developing flows these periodic conditions are achieved after a sufficient entrance length, which depends on the flow Reynolds number and geometric configuration. Streamwise-periodic flow conditions exist when the flow pattern repeats over some length L, with a constant pressure drop across each repeating module along the streamwise direction (Fluent Inc 2001). Cyclic or periodic boundary conditions are where the inflow boundary conditions are matched to the outflow boundary conditions. By specifying the inlet and outlet boundary with the cyclic boundary conditions, the calculation will iterate until the flow is fully developed (i.e. the outlet velocity profile is the same as the inflow velocity profile), ie. axial velocities U (r) are constant, and radial velocities V (r) ≈ 0. This streamwise periodic technique, with standard k-ε turbulence model and with both Fluent default and UDF law of the wall constants was used to study the developed area of flow. Fig 6 shows the solution domain geometry and adopted mesh, geometry dimensions and boundary types.

The Fluent defaults for law of the wall were considered first. The periodicity conditions were set to specify mass flow rate (kg/s) for each particular Reynolds number, and the periodic boundaries of the solution domain were set to the translational periodic type, otherwise the case files are the same as the conventional ones used before. The outputs were compared again with the experimental results of Quarmby, and the comparison is shown in Fig 7, which again shows a similar disagreement between the two results to that obtained before. Also, the comparison between periodic technique with k-ε with default values and UDF values is shown in Fig 8, which is similar to Fig 5 before.

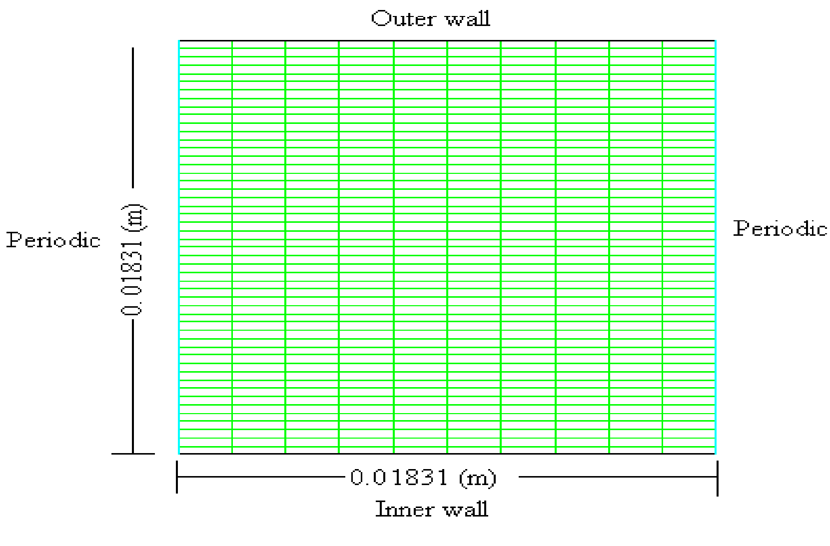

Figure 6. Streamwise solution domain geometry, adopted mesh, geometry dimensions and boundary types.

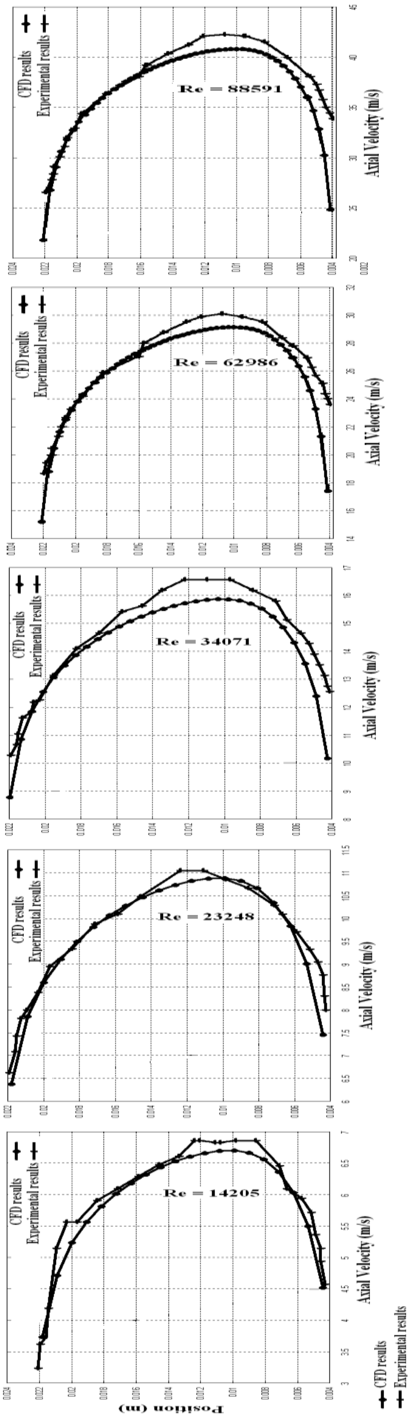

Figure 7. Comparison of periodic *k-ε* with default values and experimental results.

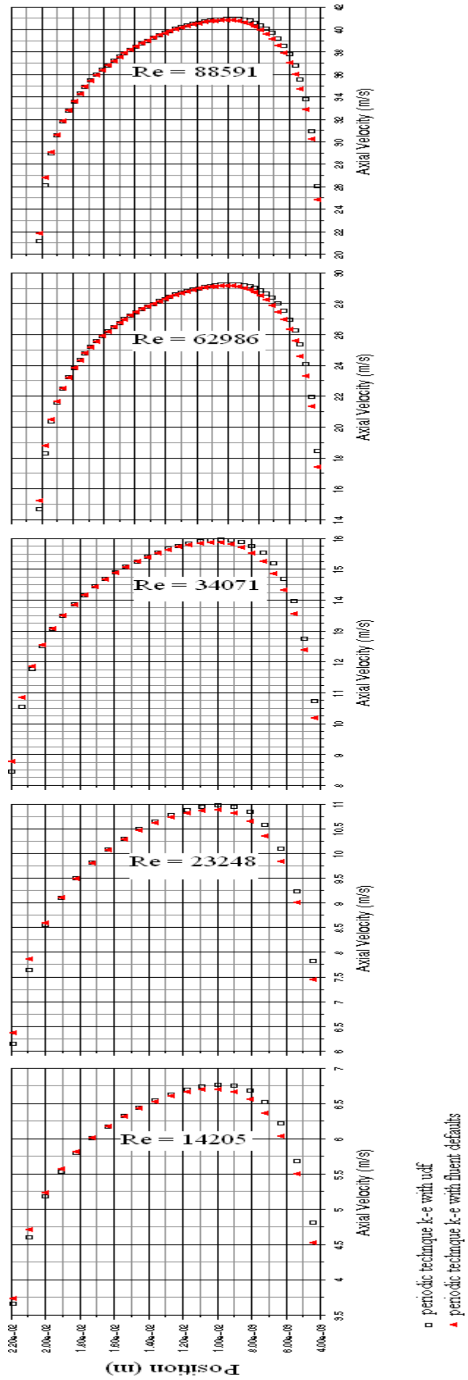

Figure 8. Comparison of periodic *k-ε* technique with fluent defaults and *k-ε* with UDF result

As an alternative, the streamwise periodic technique was implemented with *k-ω* and a very fine mesh near the wall. Fig 9 shows the solution domain, geometry and mesh. The same boundary conditions as with *k-ε* were used. The values of y^+ for this case were checked after computation and were found to be in accordance to the standard criterion of acceptable value, i.e y^+ less than one [14]. Comparisons of Fluent with *k*-*ω* and Quarmby's experimental velocity profiles are shown in Fig 10. The grid of Fig 9 gives greater resolution near the walls compared with the grid of Fig 6, which might be expected to give improved modeling of steep velocity gradient in the wall regions. However, Fig 10 shows broadly the same results as before. Marginal increments in maximum velocity values were obtained. This set of results emphasizes that the wall functions were not the key issue, since all techniques gave similar results.

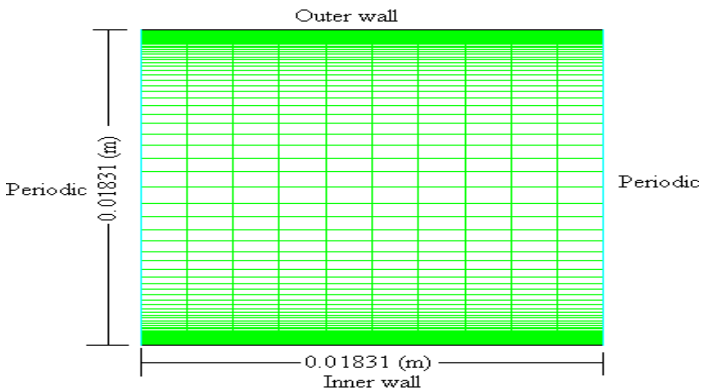

Figure 9. Streamwise solution domain, geometry, mesh and boundary types of computational model (*k*-*ω* modeling method and very fine mesh near the wall)

All approaches used so far showed difference between computational and experimental results for the maximum value of axial velocity and the velocity profiles near the inner walls, which were very pronounced at higher flow rates. Fig 8 shows, modifying the wall function contents only marginally improved the solutions, mainly at low Reynolds numbers, but still leaves inconsistency of the results for the higher Reynolds numbers cases (*Re* =34071, 62986 and 88591). Mass flow rates for these Reynolds numbers were reconsidered. Integration of the flow rates across the annulus gap for both experimental and computational profiles show some errors of the order of 3% to 3.9%. These cases were rerun with standard *k*-*ε* and experimental constants of law of the wall and the new corrected values of mass flow rates. Fig 11 shows generally a good agreement between CFD and experimental results, indicating the importance of matching computational to experimental mass flow rates. Quarmby (1967) does not give any indication of the uncertainties on his experimental results, so there would be little to gained from pursuing this comparison further.

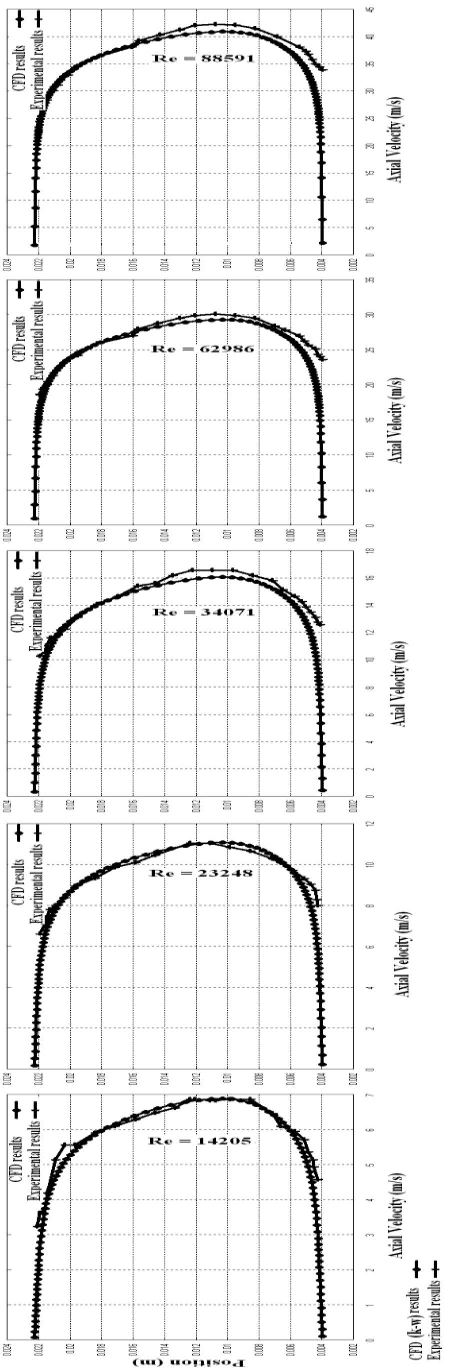

Figure. 10 Comparison of CFD (*k*-*ω*) and experimental velocity profiles.

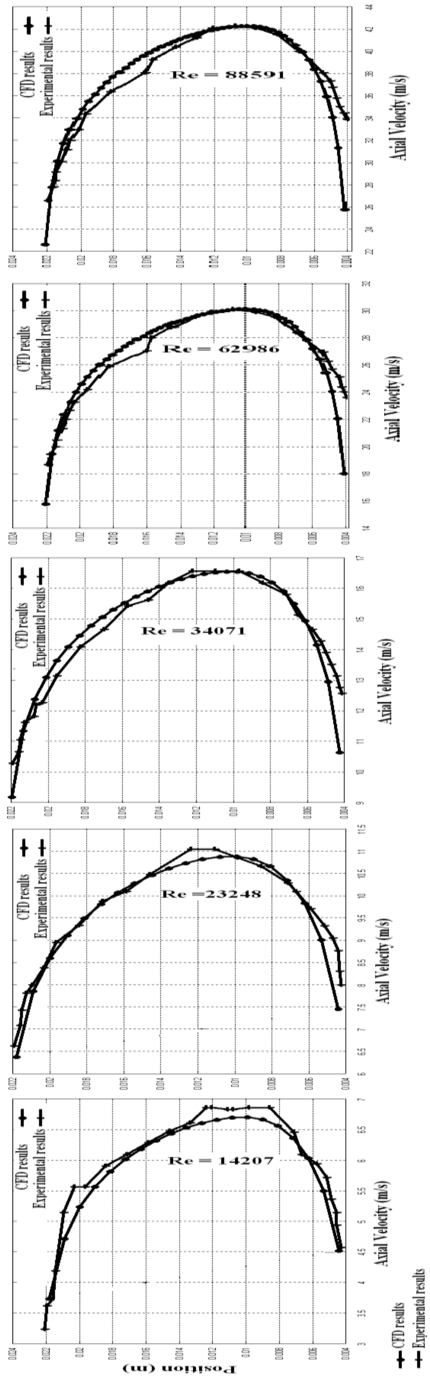

Figure. 11 Comparison of CFD (*k*-*ε*) with UDF and corrected mass flow rates and experimental velocity profile

5. Conclusion

Preliminary calculations were carried out for previously published experiments on non-swirling concentric annular pipe flow (Quarmby 1967), but computed and measured data did not reasonably match together (Fig 4, 7, 10). Notwithstanding the discussion in Quarmby (1967), implementation of user defined functions for law of the wall in a bid to match computed results of axial velocity profile with experimental results did not improve the solution. It appears that modifying the wall function constants considering experimental values has marginal effect on solution accuracy (Fig 5 and 8). Once the specified flow rates had been corrected, reasonable correlations were obtained (Fig 11).

6. References

[1] Rabia, H. (1985). Oil Well Drilling Engineering: Principles and Practice. Graham & Trotman Ltd, London.

[2] Quarmby, A. (1967). "An Experimental Study of Turbulent Flow Through Concentric Annuli." International Journal of Mechanical Science, **9**: 205-221.

[3] Fluent Inc. (2001). Fluent 6.0 Users Guide, Dec. 2001. 5 Vols, Fluent Inc, Lebanon NH, USA.

[4] Brighton, J. A. and J. B. Jones (1964). "Fully Developed Turbulent Flow in Annuli." Journal of Basic Engineering ASME, **86**: 835-844.

[5] Jonsson, V. K. and E. M. Sparrow (1966). "Experiments on Turbulent-Flow Phenomena in Eccentric Annular Ducts." Journal of Fluid Mechanics, **25**: 65-86.

[6] Smith, S. L. et al (1968). The Direct Measurement of Wall Shear Stress in an Annulus. Central Electricity Generating Board Report RD/B/N 1232**,** 1-36.

[7] Lawn, C. J. and C. J. Elliott (1971). "Fully Developed Turbulent Flow Through Concentric Annuli." Central Electricity Generating Board Rep RD/B/N 1878**,** 1-62.

[8] Kacker, S. C. (1973). "Some Aspects of Fully Developed Turbulent Flow in Non-Circular Ducts." Journal of Fluid Mechanics, **57**: 583-602.

[9] Rehme, K. (1974). "Turbulent Flow in Smooth Concentric Annuli With Small Radius Ratios." Journal of Fluid Mechanics, **64**: 263-287.

[10] Nouri, J. M. et al (1993). "Flow of Newtonian and Non-Newtonian Fluids in Concentric And Eccentric Annuli." Journal of Fluid Mechanics, **253**: 617-641.

[11] Fluent Inc (2001). Fluent 6.0 UDF Users Guide, Dec 2001. Fluent Inc Lebanon NH, USA.

[12] Potts, I. (2005). Personal Communications. School of Mechanical and Systems Engineering, Newcastle University, the UK. (unpublished).

[13] Ahmed, M. Mohamed (2006) . "Validation of CFD modeling for oil well drilling fluid flows" Ph.D. thesis, Newcastle University, the UK.

[14] Hutton, T. (2006). "Seminar Presentation: The Challenge of Turbulence Modeling in the Industrial Application of CFD.", School of Mechanical and Systems Engineering, 11 Jan. 2006 (unpublished)